Case breach fault model and diagnostic for the solid rocket

Viatcheslav V. Osipov* and Dmitry G. Luchinsky†
NASA Ames Research Center, Mail Stop 269-3, Moffett Field, CA 94035, USA and
Mission Critical Technologies Inc., 2041Rosecrans Ave. Suite 225 El Segundo, CA 90245

Vadim N. Smelyanskiy‡, Dogan A. Timucin§
NASA Ames Research Center, Mail Stop 269-2, Moffett Field, CA 94035, USA

[Abstract] A model of the case breach fault for solid rocket boosters (SRBs) that takes into account burning-through hole in propellant, insulator and metal layers of a rocket case is developed. Melting of the metal layer and an ablation of the insulator layer in the presence of hot gas flow through the hole are analyzed in detail. Dynamics of the lateral (side) thrust produced by the growing hole is calculated for typical parameters of the SRB. A problem of inference of the fault parameters from the measurements of the nominal values of stagnation pressure and thrust is formulated and solved in quasi-steady approximation. An application of the recently developed Bayesian framework for diagnostics and prognostics of the case breach fault that can cause loss of flight control is discussed.

Nomenclature

ρ	=	gas density
p	=	gas pressure
T	=	gas temperature
u	=	gas velocity
v_f	=	velocity of propagation of front of metal melting
v_{abl}	=	velocity of propagation of front of insulator ablation
c	=	sound velocity
M	=	Mach number, $M = u/c$, $M = u/c_0$
C_V	=	specific heat for the constant pressure and volume
C_P	=	specific heat for the constant pressure and volume
γ	=	ration of specific heats; $\gamma = C_p/C_V$
l	=	perimeter of propellant cross-section
e_t	=	total energy of the gas in the combustion chamber
h_t	=	total enthalpy of the gas in the combustion chamber
l_h	=	perimeter of hole cross-section
r_h	=	radius of the hole
s_h	=	cross-section of the hole
r_{hmin}	=	minimum radius of the hole
s_{hmin}	=	minimum cross-section of the hole (additional nozzle throat)
R_t	=	radius of the normal nozzle throat
S_t	=	cross section of the normal nozzle throat
L	=	length of the propellant grain
F	=	the total area of the burning surface
F_N	=	normal thrust
F_s	=	side thrust
r_b	=	burning rate of solid propellant

* Research Scientist, Mission Critical Technologies Inc. Email: osipov@email.arc.nasa.gov.
† Research Scientist, Mission Critical Technologies Inc. Email: luchinsk@email.arc.nasa.gov, AIAA member.
‡ Research Scientist, IS Division, NASA ARC. Email: Vadim.N.Smelyanskiy@nasa.gov, AIAA member.
§ Research Scientist, IS Division, NASA ARC. Email: Dogan.A.Timucin@nasa.gov

n	=	exponent for burning rate of the propellant
ρ_p	=	density of the solid propellant
H_p	=	combustion heat of the solid propellant
Q	=	heat flow from the gas to the walls of the hole
S	=	cross-section of the combustion chamber
f_{tr}	=	surface friction force
T_{mel}	=	melting temperature point
H_{met}	=	heat of combustion of case metal
T_c	=	temperature of metal case far from hole
C_{met}	=	specific heat of case metal
q_{met}	=	specific melting heat of case metal
C_{ins}	=	specific heat of insulator layer
q_{ins}	=	specific melting heat of insulator layer
ρ_{met}	=	density of case metal
ρ_{ins}	=	density of insulator layer
k	=	the thermal conductivity
μ	=	dynamical viscosity of hot gas
Pr	=	the Prandtl number, $\mathrm{Pr}=\mu C_p/k$
0	=	subscript 0 refers to the gas parameters in the combustion chamber
h	=	subscript h refers to the gas parameters in the hole

I. Introduction

In-flight diagnostics and prognostics for SRBs is an ill-posed, inverse problem, which is further complicated by the fact that the number and type of sensors available on-board are severely limited and the time window between the detectable onset of a failure and its typically catastrophic consequences is usually a few seconds. In practice, one has to infer parameters of gas flow and the grain geometry in a booster based on a few seconds' readings of 2 or 3 sensors, such as stagnation pressure and thrust. Furthermore, a number of different fault modes (including e.g. combustion instability[4,11]; local burning of the rocket case, overpressure in SRBs, and breakage of the case induced by nozzle blocking or bore choking) may lead to a similar off-nominal dynamics of SRBs. To facilitate reliable in-flight diagnostics and prognostics a number of low-dimensional performance models (LDPM) of the various fault modes in SRBs has to be developed that can be used to infer parameters of SRB dynamics and to predict time evolution of the faults. The models of SRB dynamics in various fault modes are in general stochastic and nonlinear. Therefore, the methods of dynamical inference have to be extended to allow for reconstruction of nonlinear stochastic models.

In our earlier works a novel Bayesian framework[1,2] was developed and applied for the inference of nonlinear SRB flow parameters[12-14] based on a combination of the LDPMs and stochastic simulations of the flow dynamics. In these earlier works we analyzed a few fault scenarios including: (i) step-wise nozzle blocking with progressive steady burn-out, (ii) nozzle blocking with time varying fault parameters and neutral thrust curve modeling a possible "miss" situation, where a sudden increase of pressure follows a prolonged period of small deviations of the pressure from the nominal value; (iii) model a possible "false alarm" situation where, pressure following a sudden increase, induced by a cloud of solid particles, returns to its nominal value.

In this paper we analyze the case breach fault induced by burning a hole through a rocket case. The burning case fault results in decrease both of the chamber pressure and of the normal booster thrust and also rise of lateral thrust. The additional lateral acceleration can be compensated for by the angle variation of the nozzle, TVC, but can cause loss of flight control.

A novel LPDM of the case breach fault is introduced based on detailed consideration of the melting of the metal layer and ablation of the insulator layer in the presence of hot gas flow through the hole. We show that the hole can have the form of a convergent or de Laval nozzle depending on parameters of the metal and insulator materials. A lateral (side) thrust produced by the growing hole is calculated for typical parameters of SRBs. A problem of reconstruction of the fault parameters using nominal values of stagnation pressure and thrust is formulated. We solve this problem by introducing an iterative procedure in the quasi-steady approximation. We discuss how the novel Bayesian framework can be applied for the diagnostics and prognostics of the case breach fault.

We emphasize that development of the low-dimensional models of the fault modes in SRBs is also important in a more general context of the risk analysis[3] of the space flights.

The paper is organized as follows. In Sec. II a high-fidelity model of the case breach fault is introduced and corresponding LDPM and its adiabatic approximation are derived. An analysis of the melting and ablation of the steel case and of the insulator layers is given in Sec. III. Quasi-static description of the fault and its validation using results of the numerical solution are given in Sec. IV. Finally, conclusions are drawn in Sec. V.

II. Model of the case breach fault

A. High-fidelity model of the case breach fault

To model case breach fault (see the sketch in the Fig. 1) we assume that the gas leak through the hole in the case is small compared to the gas flow through the rocket nozzle. An analysis of the fault in the limit of small gas leak is the most important one from the point of view of the development of prognostics and diagnostic of the SRB. In this case the perturbation of the gas flow in the combustion chamber is small and one can use one-dimensional approximation for both gas flow in the combustion chamber and gas flow in the hole. To describe gas flow in the combustion chamber in 1D approximation we can use a set of equations for the dynamics of mass, momentum, and the energy of the gas, introduced in our earlier work[12-14]

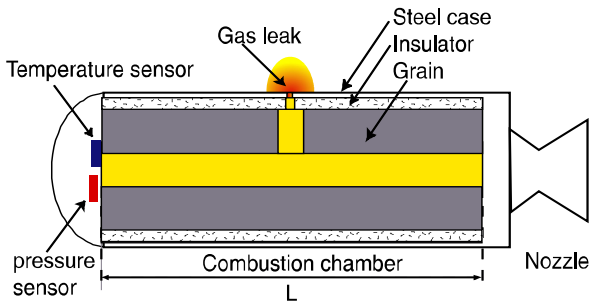

Figure 1 Sketch of an idealized geometry of the fault with a gas leak through the hole in the case.

$$\begin{cases} \partial_t\left(S\rho\right) = -\partial_x\left(S\rho u\right) + \rho_p r_b l + A_1\xi_1(t), \\ \partial_t\left(S\rho u\right) = -\partial_x\left(S\rho u^2\right) - S\partial_x p + A_3\xi_3(t), \\ \partial_t\left(S\rho e_t\right) = -\partial_x\left(S\rho h_t u\right) + H\rho_p r_b l + A_2\xi_2(t). \end{cases} \tag{1}$$

Here $\partial_t \equiv \partial/\partial t$, $\partial_x \equiv \partial/\partial x$, $e_t = c_V T + u^2/2$, $h_t = c_p T + u^2/2$ are the total energy and total enthalpy of the gas flow in the combustion chamber, $\xi_i(t)$ are white Gaussian noises with intensities A_i. This set of partial differential equations (PDE) coupled with the equation for the steady burning of the propellant

$$\frac{dR}{dt} = r_b\left(p\right) = r_c\left(\frac{p}{p_c}\right)^n = ap^n \tag{2}$$

represents a modification of the well-known work by Salita[15]. The boundary conditions for these equations assume the stagnation values for the gas parameters at the head of the rocket and the ambient conditions at the nozzle outlet. We now extend this mode by coupling the gas dynamics in the combustion chamber to the gas flow in the hole. The corresponding set of PDEs

$$\begin{cases} \partial_t\left(s_h\rho_h\right) = -\partial_x\left(s_h\rho_h u_h\right), \\ \partial_t\left(s_h\rho_h u_h\right) = -\partial_x\left(s_h\rho_h u_h^{\,2}\right) - s_h\partial_x p_h - f_{fr} l_h, \\ \partial_t\left(s_h\rho_h e_t^h\right) = -\partial_x\left[s_h\rho_h u_h h_t^h\right] - Ql_h, \end{cases} \tag{3}$$

resembles Eqs. (1). The main difference between the two sets of equations is that we neglect the mass from the walls of the hole as compared to the mass flow from the walls of the grain in the combustion chamber. Instead, Eqs. (3) include the term Ql_h that describes the heat flow from the gas to the hole walls. The boundary conditions for this set of equations assume ambient conditions at the hole outlet and the continuity equation for the gas flow in the hole coupled to the sonic condition at the hole throat. Eqs. (3) are coupled to eq. (2) and to the dynamics of the hole radius

$$\frac{dr_h}{dt} = v_f\left(r_h, p_h\right). \tag{4}$$

Here the velocity of propagation of the hole wall $v_f(r_h,p_h)$ is a complex nonlinear function of the hole curvature and the hole pressure. The derivation of the exact functional form of $v_f(r_h,p_h)$ is the key problem of the theory and will be discussed in details in the following sections. The two sets of Eqs. (1),(2) and (3),(4) are coupled to each other via values of the gas parameters at the stagnation point. It is assumed that throughout the combustion chamber and in the hole the following equation of a perfect gas holds

$$\frac{p}{\rho} = (C_p - C_V)T = \frac{p_0}{\rho_0}\left(\frac{T}{T_0}\right) = \frac{c_0^2}{\gamma}\left(\frac{T}{T_0}\right) \quad . \tag{5}$$

We now derive the corresponding low-dimensional performance model for the case breach

B. Low-dimensional model of the case breach fault

To derive the LDPM of the case breach fault we integrate equations (1) along the rocket axis to obtain[12-14] the following set of ordinary differential equations for the stagnation values of the gas parameters and the thickness of the burned propellant layer

$$\begin{cases} \partial_t\left(\rho_0 V\right) = -\left(\rho u S\right)\big|_L + \rho_p r_b(p_0)F + A_1\xi_1(t), \\ \partial_t\left(\rho_0 e_0 V\right) = -\left(\rho u S h_t\right)\big|_L + H_p\rho_p r_b(p_0)F + A_2\xi_2(t), \\ \partial_t R = r_b\left(p_0\right), \\ \partial_t r_h = v_f\left(r_h, p_0\right). \end{cases} \tag{6}$$

Here $\left(\rho u S\right)\big|_L$ and $\left(\rho u S h_t\right)\big|_L$ are the mass and the enthalpy flow from the whole burning area of the propellant including the propellant surface in the hole and p_0, ρ_0, and e_0 are the stagnation values of the flow parameters. The total mass flow from the burning propellant surface is equal to the sum of the mass flows through the nozzle' and hole throats. Assuming that sonic conditions hold both in the nozzle throat and the hole throat we obtain the following result

$$\left(\rho u S\right)\big|_L = \left(\rho_h u_h s_h\right)\big|_t + \left(\rho u S\right)\big|_t = \Gamma^{-1}\sqrt{\gamma\rho_0 p_0}\, s_{h\min} + \Gamma^{-1}\sqrt{\gamma\rho_0 p_0}\, S_t = \Gamma^{-1}\sqrt{\gamma\rho_0 p_0}\left(s_{h\min} + S_t\right) \tag{7}$$

Here $\Gamma = \left(\left(\gamma+1\right)/2\right)^{\frac{\gamma+1}{2(\gamma-1)}}$. This relation means that in the first approximation the hole is seen by the internal flow dynamics as an increase of the nozzle throat area and the dynamics of the stagnation values of the gas parameters are governed by both dynamics of the propellant burning area (related to the thickness of the burned propellant layer R) and by the hole radius r_h. The equations above have to be completed by the equations for the main thrust F_N and lateral (side) thrust F_s induced by the gas flow through the hole in the form

$$F_N = \Gamma^{-1}\sqrt{\gamma\rho_0 p_0}\, S u_{ex} + (p_{ex} - p_a)S_{ex}, \quad F_s = \Gamma^{-1}\sqrt{\gamma\rho_0 p_0}\, s_{h\min} u_{h,ex} + (p_{ex,h} - p_a)s_{h,ex}, \tag{8}$$

where p_a is ambient pressure, u_{ex} and $u_{ex,h}$ are gas velocities at the nozzle outlet and hole outlets respectively, and p_{ex} and $p_{ex,h}$ are the exit pressure at the nozzle outlet and hole outlets respectively.

C. Problem of reconstruction of the fault parameters and quasi-steady approximation

The problem of prognostics and diagnostics of the fault modes of SRBs is to reconstruct fault parameters from the measurements of the head (stagnation) pressure and thrust and to use inferred values of the fault parameters to predict gas flow dynamics. The results obtained above indicate that equations (6)-(8) provide a convenient framework for the solution of this problem because they directly relate measured values to the fault parameters. The difficulty in the solution of this problem is the fact that the inference of the fault parameters has to be done from the actual and nominal measurements of the p_0, F, and F_s under the assumption that the information about other details of the internal flow is not available. To solve this problem, we notice that Eqs. (6) can be further simplified because the characteristic time scales for the burning of the propellant surface and of the hole walls are much slower than the characteristic time scales of the equilibration of the flow in the combustion chamber. This assumption is well satisfied for realistic parameters of SRBs[12-14,16]. Under this assumption the time derivatives in the first two equations can be set to zero. As a result the following relation for the stagnation pressure can be obtained

$$p_0(t) = \left[\frac{\rho_p c_0 \Gamma F r_c}{\gamma p_x^n S_{ef}} \right]^{\frac{1}{1-n}} \tag{9}$$

where $S_{ef}=s_{h,t}+S_t$ is the effective area of the nozzle throat and F_{ef} is the total area of the burning surface. Therefore, under the conditions of quasi-steady burning the LDPM of the case breach fault is now reduced to the following form

$$p_0(t) = \left[\frac{\rho_p c_0 \Gamma F r_c}{\gamma p_x^n S_{ef}} \right]^{\frac{1}{1-n}}, \quad \partial_t R = r_b\left(p_0\right), \quad \partial_t r_h = v_f\left(r_h, p_0\right). \tag{10}$$

The parameters of the fault (in this case the functional form of the nonlinear time variation of the hole radius $r_h(t)$ at the hole throat and hole outlet) have to be inferred using nominal dynamics of the gas parameters. Under quasi-steady burning conditions the nominal model has a form similar to the set of Eqs. (10), except that the $v_f = 0$. It is clear that to solve the problem of reconstruction of the parameters of the case breach fault one has to know the functional form of the velocity $v_f\left(r_h, p_0\right)$. The derivation of the functional form for the $v_f\left(r_h, p_0\right)$ is, therefore, the key theoretical problem of the case breach diagnostics and prognostics. We will now describe briefly the results of the theoretical analysis of the melting of the metal case and ablation of the insulator layer in the presence of the hot gas flow through the hole.

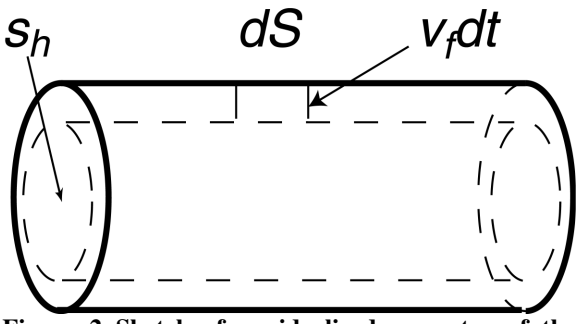

Figure 2 Sketch of an idealized geometry of the fault with a gas leak through the hole in the case.

III. Theory of the melting and ablation of the metal and insulator layers

A. Velocities of melting and ablation

Rocket cases consist of metal and insulator layers. The radius of a hole in the metal layer is determined by melting of the metal surface under the action of hot gas flow from the combustion chamber, $J = s_h \rho u$. The gas parameters in the hole can be described by the hydrodynamic Eqs. (3). In these equations $f_{fr} = \alpha \rho u^2$, α is coefficient friction between the gas flow and the metal surface; $Q = Q_c + Q_R$, $Q_c = h_g(T_g - T_{mel})$ and Q_R are convective and radiant heat flows from hot gas to the metal surface, h_g is the convective heat transfer coefficient. The velocity of propagation of the melting front v_f is determined by the equation of the heat balance for a small element of the hole surface dS (Fig. 2):

$$QdSdt = \left[q_t + q_{heat}^{met} \right] \rho_m v_f dSdt \tag{11}$$

where dt is a small time interval and $q_{heat}^{met} = C_{met}\left(T_{mel} - T_c\right)$ is the energy supplied for heating of the metal mass unit to the melting temperature T_{mel}. Thus

$$v_f = \frac{Q}{\left[q_{met} + q_{heat}^{met} \right] \rho_m} = \chi_{met}\left[h_g(T - T_{mel}) + Q_R \right], \quad \chi_{in}^{-1} = \left[q_{met} + q_{heat}^{met} \right] \rho_m \tag{12}$$

Calculations show that the thin surface layer of melted metal is ejected from the hole under the action of the hot gas flow moving with typical velocity $u = c_* \simeq 10^3 m/s$ for very short time. The time of the ejection is approximately equal to $\tau = L_h / v_{enj} < 10^{-5} s$ for a hole length $\mathrm{L_h} < 0.1\mathrm{m}$, where $v_{enj} = \dfrac{\alpha \rho_* c_*^2}{\rho_m v_f} \simeq 10^4 cm/s$ and

$\alpha \geq 0.01$. Thus, v_f is the velocity of motion of the hole surface in the metal layer. The metal surface can react with active components of the gas (combustion products). This effect can influence the hole growth if the ignition temperature $T_{ig}<T_{mel}$.

The hole in the insulator layer is determined by ablation of the insulator material at the hole surface under the action of the hot gas flow. The velocity of propagation of the ablation front v_{abl} is determined by an equation analogous to Eq. (6)

$$v_{abl} = \frac{Q}{\left(q_{abl} + q_{heat}^{ins}\right)\rho_{in}} = \chi_{in}\left[h_g(T_g - T_{abl}) + Q_R\right], \quad \chi_{in}^{-1} = \left(q_{abl} + q_{heat}^{ins}\right)\rho_{in} \tag{13}$$

where $q_{heat}^{ins} = C_{in}\left(T_{abl} - T_c\right)$ is the energy supplied for heating the insulator mass unit to the temperature T_{abl}. The coefficient of heat transfer h_g from a hot gas flow to the insulator or metal surface is given by Bartz`s equation[8-10,19,20]

$$h_g = A\left(\rho v\right)^{1-\beta} C_p\left(\Pr\right)^{-0.67}\left(\frac{2r_h}{\mu}\right)^{-\beta} \tag{14}$$

where $A = 2.3\times10^{-2}$, $\beta = 0.2$, ρv is the gas flow averaged over the hole cross-section, $\Pr = \mu C_p / k \simeq 1$ is the Prandtl number[6,8], r_h is minimum radius of the hole, k is the thermal conductivity and μ is the dynamical viscosity of the hot gas. The hole is an additional nozzle and its minimum cross section $s_{hmin} = s_{h*}$ is the nozzle throat[13,20]. Therefore, the gas flow and temperature inside the hole throat are equal to[8,9]

$$J = \rho v s_h = \rho_* c_* s_{hmin} = \rho_0 c_0 s_{hmin}\Gamma^{-1} = \frac{\gamma p_0}{\Gamma c_0} s_{hmin}, \quad T_t = T_* = \frac{2T_0}{\gamma+1}, \quad \Gamma = \left(\frac{\gamma+1}{2}\right)^{\frac{\gamma+1}{2(\gamma-1)}}. \tag{15}$$

Here we took into account that the pressure in the combustion chamber is greater than the atmospheric pressure, therefore the gas flow density $j = \rho v$ in the hole throat is equal to its maximum value[8,9]

$j_{\max} = \rho_* c_* = \rho_0 c_0 \Gamma^{-1} = \gamma p_0 / \Gamma c_0$. It follows from Eqs. (14) and (15)

$$h_g = h_g(p_m)\left(\frac{\rho v \Gamma p_0}{\rho_0 c_0 p_m}\right)^{1-\beta}\left(\frac{r_{h0}}{r_h}\right)^{\beta}, \quad h_g(p_m) = A\left(\frac{\gamma p_m}{\Gamma c_0}\right)^{1-\beta} C_p\left(\Pr\right)^{-\alpha}\left(\frac{2r_{h0}}{\mu}\right)^{-\beta} \tag{16}$$

Here r_{h0} is an initial radius of the hole and p_m is the maximum pressure in the combustion chamber.

Estimations show that $Q_c \gg Q_R$ for typical parameters of the hot gas. Therefore, we will neglect the radiant heat Q_R assuming $Q = Q_c$. In this case Eqs. (13) with the use of Eq. (16) can be written as

$$v_f(t) = v_{fm}\left(\frac{\rho v \Gamma p_0(t)}{\rho_0 c_0 p_m}\right)^{1-\beta}\left(\frac{r_{met}(t,x)}{r_{met0}}\right)^{-\beta}\left(\frac{T - T_{mel}}{T_* - T_{mel}}\right) \tag{17}$$

where

$$v_{fm} = \chi_{mel} h_g(p_m)\left(T_* - T_{mel}\right) \tag{18}$$

and Eqs. (13) and (7) can be presented as

$$v_{abl}(t) = v_m\left(\frac{\rho v \Gamma p_0}{\rho_0 c_0 p_m}\right)^{1-\beta}\left(\frac{r_{ins}(t,x)}{r_{ins0}}\right)^{-\beta}\left(\frac{T - T_{abl}}{T_* - T_{abl}}\right) \tag{19}$$

where

$$v_m = \chi_{inl} h_g(p_m)\left(T_* - T_{abl}\right) \tag{20}$$

r_{met} and r_{ins} are the radii of the holes in the metal and insulator layers, respectively, and r_{met0} and r_{ins0} are the initial values of the radii. The radius of a cylindrical or conical hole and its cross section in the metal and insulator layers are equal respectively to

$$r_{met} = r_{met0}(x) + \int_{t_0}^{t} v_f(\tau, x) d\tau, \quad s_{met}(x,t) = \pi r_{met}^2 \tag{21}$$

$$r_{ins} = r_{ins0}(x) + \int_{t_0}^{t} v_{abl}(\tau, x) d\tau, \quad s_{ins}(x,t) = \pi r_{ins}^2 \tag{22}$$

We notice above that the hole is an additional nozzle with a throat that is determined by the minimum cross section of the hole, s_{hmin}. Therefore, the gas pressure in the combustion chamber in a rocket with a hole is equal to[12,13]

$$p_0(t) = p_{00}(t) \left[\frac{S_t \left(F_0 + \Delta F \right)}{\left(S_t + s_{h\min}(t) \right) F_0} \right]^{\frac{1}{1-n}} \tag{23}$$

where $p_{00}(t)$ is the pressure in a rocket without a hole, and n is the exponent in the well-known equation for the burning rate of the propellant

$$v_b = v_{bm} (p / p_m)^n \tag{24}$$

Typical values are $n = 0.35$ and $r_{bm} = 1cm/s$ for gas pressure $p_m = 1000 psi$. According to (23) the relative decrease of the pressure $\frac{\Delta p}{p_{00}(t)} = \frac{p_{00}(t) - p_0(t)}{p_{00}(t)} \simeq \frac{s_{h\min}}{(1-n)S_t}$ is greater than 0.1% only when the hole has a large enough radius $r_h > 0.03R_t$, i.e. $r_h > 3cm$ at $R_t \simeq 1m$.

B. Influence of metal melting and surface friction on gas parameters inside the hole

Analysis of Eqs. (3), (5) shows that the effects of metal melting and surface friction are negligible for a hole radius $r_h \gg 0.005L$ where L is length of the hole. This condition is certainly valid for $r_h > 0.03R_t$. Let us explain this claim. The heat flow of the hot gas through a hole during the time dt is equal to $dQ_g = C_p T \rho \pi r_h^2 u dt$ and the heat flow spent for metal melting is $dQ_{met} = \left[q_{met} + q_{heat}^{met} \right] \rho_{met} 2\pi L_h r_h v_f dt$. Here L_h and r_h are the length and radius of the hole in the metal case. The melting is negligible when $dQ_g \gg dQ_m$. Taking into account that the gas flow density inside the hole $j = \rho u = \rho_* c_*$, $T = T_*$ and $v_f \simeq 0.1 cm/s$ this condition is reduced to

$$\frac{L_h}{r_h} \ll \frac{C_p T_* \rho_* c_*}{2\left[q_t + q_{heat}^{met} \right] \rho_{met} v_f} \simeq 900 \tag{25}$$

or $r_h \gg L_h / 900 \simeq 3\times10^{-3} cm$ at a hole length L_h=2.5cm. In other words, the hole radius has to be greater than $0.03mm$. The friction induced decrease of the pressure in the hole (axis x is directed to outside) is approximately

$$p(x) = \frac{p_*}{1 + \gamma(1 + 2\alpha x / r_h)} \tag{26}$$

Thus, when a hole radius $r_h >> r_{cr} = 2\alpha L$ the friction is negligible. The value of $r_{cr} \gg 5\times10^{-2}$cm for L=2.5cm and $\alpha = 0.01$.

C. Iteration procedure for the solution of inverse problem

We are now ready to present the solution of the inverse problem posed in the end of the previous section. Let us first to summarize the set of equations that have to be solved. For the sake of simplicity we will consider the case when the change of the burning surface area due to the change of the pressure was neglected. We show now how the dynamics of the hole radius can be reconstructed using measurements of pressure. For convenience we rewrite Eqs. (17) and (23) below

$$v_f(t) = v_{fm}\left(\frac{p_0}{p_m}\right)^{1-\beta}\left(\frac{r_{met}(t,x)}{r_{met0}}\right)^{-\beta}, \quad s_{met}(x,t) = \pi r_{met}^2$$

$$r_{met} = r_{met0}(x) + \int_{t_0}^{t} v_f(\tau, x)d\tau, \quad p_0(t) = p_{00}(t)\left[\frac{S_t}{(S_t + s_{met}(t))}\right]^{\frac{1}{1-n}}$$

The problem is to reconstruct $r_{met}(t)$ using measurements of the $p_0(t)$ and $p_{00}(t)$. To solve this problem we introduce the following iteration procedure

1. Calculate the pressure:. $p_0^i(t) = p_{00}\left(\frac{S_t}{S_t + s_{hi}}\right)^{\frac{1}{1-n}}$
2. Solve iteratively equation $\xi_i(t) = \left(1 + \int_{t_0}^{t} \xi_i(\tau)\sigma_i(\tau)d\tau\right)^{-\beta}$, where

   $\sigma_i(\tau) = \frac{v_{fm}}{r_{met0}}\left(\frac{p_0^i}{p_m}\right)^{1-\beta}$ and $\xi_i(t) = \left(\frac{r_{met}^i}{r_{met0}}\right)^{-\beta}$.
3. $s_{met}^i = \pi\left(r_{met}^i\right)^2$

The iterative procedure 1, 2, and 3 above can be applied at each time step t yielding required values of the $r_{met}(t)$. The results of the calculation of these calculations can be used to reconstruct the lateral and main thrust of the rocket using Eqs. (8). Further discussion of the thrust calculations is given in Sec. III, 0. We now consider in detail various scenarios of the dynamics of the hole shape the quasi-static approximation.

IV. Quasi-static description of the fault

We use the well-known quasi-static approximation for a description of the case breach fault due to a slow change of gas pressure in the combustion chamber, $p_0(t)$, with a negligible influence of metal melting, insulator ablation, and surface friction on the gas flow in the hole. According to this thermodynamic approximation, the gas pressure, density, temperature, and sound velocity in the stationary state are equal to[6,7]

$$p = p_0\left[\left(1 - \frac{(\gamma-1)}{2}M_0^2\right)\right]^{\frac{\gamma}{\gamma-1}} = p_0\left(1 + \frac{(\gamma-1)}{2}M^2\right)^{\frac{-\gamma}{\gamma-1}}, \tag{27}$$

$$\rho = \rho_0\left[\left(1 - \frac{(\gamma-1)}{2}M_0^2\right)\right]^{\frac{1}{\gamma-1}} = \rho_0\left(1 + \frac{(\gamma-1)}{2}M^2\right)^{\frac{-1}{\gamma-1}}, \tag{28}$$

$$T = T_0\left(1 - \frac{(\gamma-1)}{2}M_0^2\right) = T_0\left(1 + \frac{(\gamma-1)}{2}M^2\right)^{-1}, \tag{29}$$

$$c = c_0\left[\left(1 - \frac{(\gamma-1)}{2}M_0^2\right)\right]^{\frac{1}{2}} = c_0\left(1 + \frac{(\gamma-1)}{2}M^2\right)^{-\frac{1}{2}}. \tag{30}$$

Where $c = \sqrt{\gamma p/\rho}$ is a sound velocity and $c_0 = \sqrt{\gamma p_0/\rho_0} = \sqrt{C_p(\gamma-1)T_0}$ is the sound velocity in the combustion chamber; $M = u/c$ is the Mach number, $M = u/c_0$, u is the gas velocity; p_0, T_0 and ρ_0 are the gas parameters in a combustion chamber.

Estimations show that the velocities of the propagation fronts of metal melting and insulator ablation given by Eqs. (13), (17) and (13), (19) are approximately equal for typical parameters of metal and insulator materials, $v_f \approx v_{abl} \approx 0.1 cm/s \ll r_{bm}$. Therefore, two typical scenarios shown in Fig. 3 that can occur depending on the parameters of the metal (steel) and insulator materials.

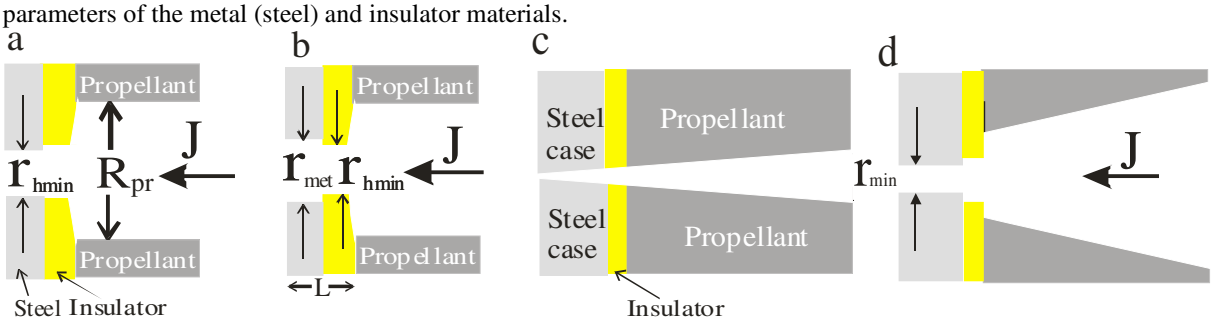

Figure 3 Possible profiles of holes in a rocket case at a time point $t > t_0$: (a) hole in the form of a convergent nozzle for $v_f < v_{abl}$; (b) hole in the form of a de Laval nozzle for $v_f > v_{abl}$, the holes (a) and (b) had the cylindrical geometry with an initial radius $r_{h0} < r_{h\min}$ at the start time of the fault $t = t_0$; (c) and (d) cone-shaped profiles of a hole at the start time of the fault $t = t_0$ and $t > t_0$, respectively. $J = \rho_* c_* s_{h\min}$ is the hot gas flow in the hole effluent from the combustion chamber.

A. Comparison with the results of high-fidelity simulations

To validate the quasi-static description of the fault we performed high-fidelity simulations of the case breach fault using FLUENT[22]. The simplified geometry of the fault with cylindrically-symmetrical is shown in Fig. 4.

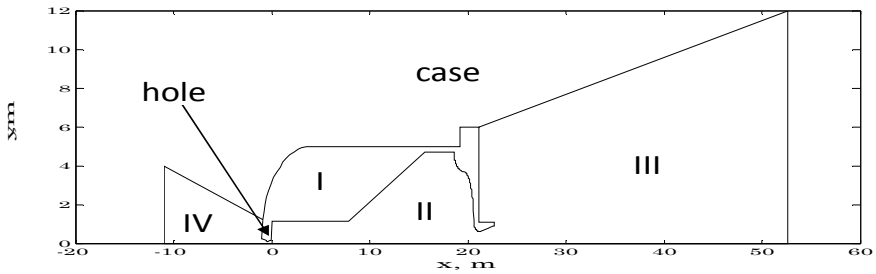

Figure 4 Simplified geometry of the fault with the case breach fault at the head of the rocket. I – propellant; II – combustion chamber; III – ambient region; IV – ambient region for the fault at the head of the rocket.

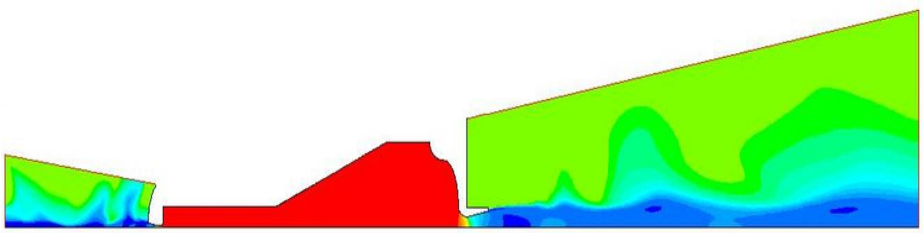

Figure 5 Distribution of the gas density in the combustion chamber, nozzle, the hole through the case, and in the ambient regions near the case breach fault and the nozzle obtained using FLUENT.

The hole through the case is situated in the head of the rocket. The results of the simulations are shown in Fig.5. It can be seen from the figure that the sonic conditions are hold for both the nozzle throat and the hole throat.

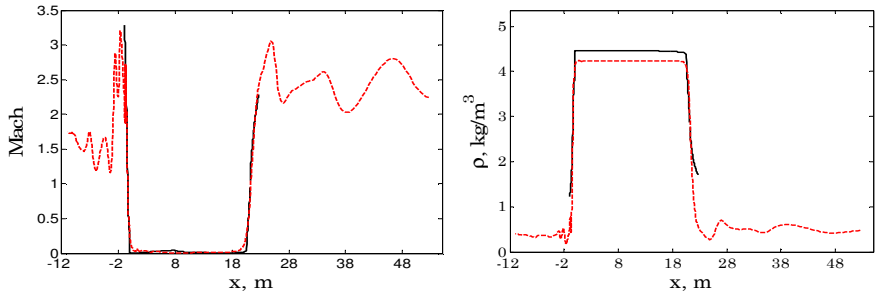

Figure 6 (left) Mach number obtained using analytical results for stationary 1D approximation (solid black line) and using FLUENT (red dashed line) along the rocket axis. (right) The density obtained using analytical results for a stationary 1D approximation (solid black line) and using FLUENT (red dashed line) along the rocket axis.

The comparison between the results of the results of FLUENT simulations and the theory presented in the previous sections is shown in Fig. 5.

It can be seen from the figure that the quasi-static theory of the axial dependence of the Mach number and of the density describes very well the actual variation of the gas flow parameters along the rocket axis. Some deviations of the results of simulations from the predicted values in the ambient regions are attributed to the slow convergence of the simulations and will be investigated in more detail elsewhere.

The comparison between the results of the results of FLUENT simulations and the theory presented in the previous sections is shown in Fig. 6.

It can be seen from the figure that the quasi-static theory of the axial dependence of the Mach number and of the density describes very well the actual variation of the gas flow parameters along the rocket axis. Some deviations of the results of simulations from the predicted values in the ambient regions are attributed to the slow convergence of the simulations and will be investigated in more detail elsewhere.

B. Burn-through hole in the form of a convergent nozzle

Estimations show that probably $v_f < v_{abl}$ and the gas flow is limited by the cross section of the hole in the metal layer, i.e. $s_{h\min} = s_{met}$. In this case the hole in the metal layer is the throat of an additional convergent nozzle, Fig. 3a. In such a throat[6,7] the gas pressure, density, temperature, and velocity are equal respectively to

$$p_* = p_0\left(\frac{2}{\gamma+1}\right)^{\frac{\gamma}{\gamma-1}}, \quad \rho_* = \rho_0\left(\frac{2}{\gamma+1}\right)^{\frac{1}{\gamma-1}}, \quad T_* = T_0\left(\frac{2}{\gamma+1}\right), \quad c_* = c_0\left(\frac{2}{\gamma+1}\right)^{\frac{1}{2}}. \tag{31}$$

The gas flow through the hole according to Eqs. (15)and (31) is

$$J = \rho u \mathrm{s_h} = \rho_* c_* \mathrm{s_{hmin}} = \rho_0 c_0 s_{met} \Gamma^{-1} \tag{32}$$

With the use of Eqs. (31) and (32), the equations (11) and (19)are reduced to

$$v_f(t) = v_{fm}\left(\frac{p_0}{p_m}\right)^{1-\beta}\left(\frac{r_{met}(t,x)}{r_{met0}}\right)^{-\beta}, \tag{33}$$

$$v_{abl}(t) = v_m\left(\frac{\Gamma p_0}{p_m}\right)^{1-\beta}\left(\frac{r_{ins}(t,x)}{r_{ins0}}\right)^{-\beta}\left(\frac{T-T_{abl}}{T_*-T_{abl}}\right)\mathrm{M}_0^{1-\beta}\left(1-\frac{\gamma-1}{2}M_0^2\right)^{\frac{1-\beta}{\gamma-1}} \tag{34}$$

where T is determined by Eq. (29) and M_0 is a minimum root of the equation

$$\mathrm{M}_0\left(1-\frac{(\gamma-1)}{2}M_0^2\right)^{\frac{1}{\gamma-1}} = \frac{s_{met}}{\Gamma s_{ins}} \tag{35}$$

This equation follows from Eqs. (28) and (32).

In the considered case the exhaust gas parameters of an additional convergent nozzle are equal to $p_{ex} = p_*$, $u_{ex} = c_*$, and $J_{ex,h} = \rho_* c_* \mathrm{s}_{\mathrm{met}} = \dfrac{\gamma p_0}{\Gamma c_0} \mathrm{s}_{\mathrm{met}}$. Therefore, the side thrust is given by the following equations:

$$F_s = J_{ex,h} u_{ex,h} + (p_{ex} - p_a) s_{met} = \frac{\gamma p_0 c_*}{\Gamma c_0} s_{met} + (p_* - p_a) s_{met} = \left(\frac{2}{\gamma+1}\right)^{\frac{\gamma}{\gamma-1}} (1+\gamma)\, p_0 s_{met} - p_a s_{met} \quad (36)$$

The main rocket thrust is determined by

$$F_N = J_{ex} u_{ex} + (p_{ex} - p_a) S_{ex} = \left[\frac{\gamma}{\Gamma} S_t M_{ex} + S_{ex}\left(1 - \frac{(\gamma\text{-}1)}{2} M_{ex}^2\right)^{\frac{\gamma}{\gamma-1}}\right] p_0 - p_a S_{ex}, \quad (37)$$

where $J_{ex} = \rho_* c_* S_t = \dfrac{\gamma p_0}{\Gamma c_0} S_t$, p_0 is given by Eq. (23) with $s_{h\min} = s_{met}$ and M_{ex} is a maximum root of the equation

$$\mathrm{M}_{\mathrm{ex}}\left(1 - \frac{(\gamma\text{-}1)}{2} M_{ex}^2\right)^{\frac{1}{\gamma-1}} = \frac{S_t}{\Gamma S_{ex}} \quad (38)$$

where S_{ex} is the exhaust cross section of the nozzle. Eq. (37) can be written as

$$F_N = \left[\frac{\gamma}{\Gamma} M_{ex} + \left(\frac{1}{\Gamma M_{ex}}\right)^{\gamma} \left(\frac{S_t}{S_{ex}}\right)^{\gamma-1}\right] p_0 S_t - p_a S_{ex}, \quad (39)$$

where $s_{h\min} = s_{met}$. During the active part of booster flight $p_0 \gg p_a$. Therefore, we find from Eqs. (37) and (39)

$$\frac{F_s}{F_N} = \left(\frac{2}{\gamma+1}\right)^{\frac{\gamma}{\gamma-1}} \left[\frac{\gamma}{\Gamma} M_{ex} + \left(\frac{1}{\Gamma M_{ex}}\right)^{\gamma} \left(\frac{S_t}{S_{ex}}\right)^{\gamma-1}\right]^{-1} \frac{(\gamma+1) s_{h\min}}{S_t} \quad (40)$$

It follows from Eq. (40) that the side thrust is determined by the minimum cross section of the hole and $F_s / F_N \simeq 7 s_{h\min} / S_t$ for typical values ($\gamma = 1.3 - 1.4$, $M_{ex} \simeq 2$, $S_{ex} \simeq (3 \div 6) S_t$. This means that $F_s / F_N \geq 1\%$ when the hole radius $r_{h\min} \geq 0.04 R_t$, i.e. $r_{h\min} \geq 10 cm$ at $R_t = 2.5 m$.

According to Eq. (18), the radius and cross section of the hole in the propellant are given

$$r_{pr} = r_{pr0}(x) + \int_{t_0}^{t} r_{cm} \left(\frac{p(x,t)}{p_m}\right)^n d\tau, \quad S_{pr}(x,t) = \pi r_{pr}^2 \quad (41)$$

where, as it follows from Eqs. (27), (28), and (32), the pressure is determined by the equations

$$p = p_0 \left[\left(1 - \frac{(\gamma-1)}{2} M_{pr}^2\right)\right]^{\frac{\gamma}{\gamma-1}}, \quad \mathrm{M}_{\mathrm{pr}}\left(1 - \frac{(\gamma\text{-}1)}{2} M_{pr}^2\right)^{\frac{1}{\gamma-1}} = \frac{s_{h\min}}{\Gamma S_{pr}}. \quad (42)$$

Taking into account that $s_{h\min} \ll \Gamma S_{pr}$ we find that

$$p(x,t) = p_0(t)\left(1 - \frac{(\gamma-1)}{2}\left[\frac{s_{n\min}(x,t)}{\Gamma S_{pr}(x,t)}\right]^2\right)^{\frac{\gamma}{\gamma-1}} \quad (43)$$

Thus, the pressure in the propellant hole $p(x,t)$ is very close to $p_0(t)$ and $r_{pr} \simeq r_{pr0}(x) + \int_{t_0}^{t} r_{cm} \left(\frac{p_0(t)}{p_m} \right)^n d\tau$.

C. Burn-through hole in the form of a de Laval nozzle

In the case $v_f > v_{abl}$ the gas flow will be limited by the cross section of the hole in the insulator layer, $s_{h\min} = s_{ins}$ and the geometry of the burn-through hole resembles the form of a de Laval nozzle with an exhaust gas velocity $u_{ex} > c \quad (M > 1)$. The hole in the insulator layer is the throat of this additional nozzle, Fig. 3b. In such a throat[8,9] the gas pressure, density, temperature, and velocity are determined by Eqs. (31). It follows that

$$v_{abl}(t) = v_m \left(\frac{p_0}{p_m} \right)^{1-\beta} \left(\frac{r_{ins}(t,x)}{r_{ins0}} \right)^{-\beta} \tag{44}$$

$$v_f(t) = v_{fm} \left(\frac{\Gamma p_0}{p_m} \right)^{1-\beta} \left(\frac{r_{met}(t,x)}{r_{met0}} \right)^{-\beta} \left(\frac{T - T_{mel}}{T_* - T_{mel}} \right) \mathrm{M}_0^{1-\beta} \left(1 - \frac{\gamma - 1}{2} M_0^2 \right)^{\frac{1-\beta}{\gamma-1}} \tag{45}$$

where T is determined by Eq. (29) and M_0 is a maximum root of the equation

$$M_0 \left(1 - \frac{\gamma - 1}{2} M_0^2 \right)^{\frac{1}{\gamma-1}} = \frac{s_{ins}}{\Gamma s_{met}} \tag{46}$$

In the considered case, the exhaust gas parameters of the additional convergent nozzle are equal to

$$J_{ex} = \rho_* c_* \mathrm{s}_{\mathrm{ins}} = \frac{\gamma p_0}{\Gamma c_0} \mathrm{s}_{\mathrm{ins}}, \; p_{ex} = p_0 \left(1 - \frac{\gamma - 1}{2} M_0^2 \right)^{\frac{\gamma}{\gamma-1}}, \; u_{ex} = c_0 M_0 . \tag{47}$$

Therefore, the side thrust is given by the following equations:

$$F_s = J_{ex} u_{ex} + (p_{ex} - p_a) s_{met} = \left[\frac{\gamma}{\Gamma} s_{ins} M_0 + s_{met} \left(1 - \frac{\gamma - 1}{2} M_0^2 \right)^{\frac{\gamma}{\gamma-1}} \right] p_0 - p_a s_{met} =$$
$$\left[\frac{\gamma}{\Gamma} M_0 + \left(\frac{1}{\Gamma M_0} \right)^{\gamma} \left(\frac{s_{ins}}{s_{met}} \right)^{\gamma-1} \right] p_0 s_{ins} - p_a s_{met} \tag{48}$$

where p_0 and M_0 are given by Eqs. (23) with $s_{h\min} = s_{ins}$ and (46), respectively. Relationship F_s / F_N is determined by Eqs. (37) and (48) where $s_{h\min} = s_{ins}$. In this case F_s / F_N is almost proportional to $s_{h\min} / S_t$. The radius and cross section of the hole in the propellant are determined by Eqs. (41)-(43) where $s_{n\min} = s_{ins}$.

D. Evolution of burn-through hole of complex forms

The hole can be a crack of cone-shaped profile passing through the propellant, insulator, and metal layers, Fig. 3c. In this case the pressure and the hot gas flow density, according to Eq. (15), will drop as $\rho u = \rho_* c_* s_h(x) / s_{h\min} \propto r_h^2$ with decrease of the hole radius. It follows from Eqs. (17) and (19) that the velocities of metal melting and insulator ablation will increase towards the rocket case surface. It means that the wedge-shaped hole will reduce to a cylindrical form as shown in Fig. 3d. On the contrary the hole in propellant will look more cone-shaped due to the decrease of the pressure.

The crack can have an elliptical cross section, In this case, the radius r_h in Eqs. (17) and (19) has to be used a a substitute for the radius of curvature of the surface. As a result eccentricity of the ellipsis will now increase as is shown in Fig. 7.

Thus, we see that evolution of a cone-shaped elliptic hole has an intricate behavior. At the same time the main characteristics, the change of the pressure and thrust, are determined only by the dynamics of growth of the minimum cross section of the hole and does not depend on the actual shape of the hole. In particular, the relationship between the main and side trusts according to Eq. (40) is determined only by $s_{h\min}$. Therefore, measurement of this relationship can be used as additional information for an analysis of the fault. The time-dependence of $s_{h\min}(t)$ can be predicted on the basis of the noisy dynamics and analysis of data of the pressure and acceleration sensors and angle variation of the nozzle based on the novel dynamical method for in-flight diagnostics and prognostics of SRBs parameters. This will allow us to predict the time moment when the side trust can reach a critical value and the flight can lose control. This work is in progress.

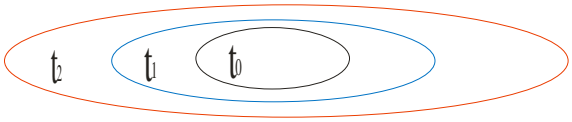

Figure 7 Sketch of an idealized geometry of the fault with a gas leak through the hole in the case.

V. Conclusion

We developed the high-fidelity model of the case breach fault based on a system of stochastic partial differential equations for momentum, energy and mass of combustion products (gas) averaged over a cross-section area. The model takes into account gas leak through a hole in rocket case, fluctuations of the burning rate, and is suitable for simulations of an arbitrary thrust curve for graded propellants. The corresponding low-dimensional model of the propellant performance was derived using the introduced system of PDEs. A theory of the front propagation of the metal and insulator layers was developed. A self-consistent analysis of the hole dynamics in the propellant, insulator and metal layers of a rocket case was performed for various parameters. One of the most dangerous effects of the case breach fault is the rise of lateral (side) thrust as a result of the growing hole. We showed that variations of the chamber pressure and the value of the normal and side thrusts are determined by dynamics of minimum cross section of the hole but do not depend on its shape.

A problem of reconstruction of the fault parameters from the measurements of the nominal and off-nominal values of the chamber pressure was formulated. We developed an iterative procedure of solution of this inverse problem. We note that obtained in this work low-dimensional performance model allows one to apply recently developed Bayesian framework for diagnostics and prognostics of the case breach fault. In particular, the prognostics of the case breach fault, based on the real-time analysis of sensor data, can be used to determine the time moment when the fault causes the loss of the flight control. This work is progress.

Acknowledgments

We deeply appreciate fruitful discussions with Dr. Matthew Cross (NASA MSFC).

References

Periodicals

[1]Smelyanskiy,V.N., Luchinsky D.G., Timuçin D. A., and Bandrivskyy A., "Reconstruction of stochastic nonlinear dynamical models from trajectory measurements", *Physical Review E*, Vol. 72, No. 2, 2005, 026202.

[2]V. N. Smelyanskiy, D. G. Luchinsky, A. Stefanovska, and P. V. E. McClintock, "Inference of a Nonlinear Stochastic Model of the Cardiorespiratory Interaction", *Phys. Rev. Lett.* Vol. 94, No. 9, Mar. 2005, 098101.

[3]Seife, C., "SPACE SHUTTLE: Columbia Disaster Underscores the Risky Nature of Risk Analysis", *Science,* Vol. 299. No. 5609, Feb 2003, pp. 1001 – 1002.

Books

[4]Culick, F.E.C., *Combustion of the Stability in Propulsion System*, Unsteady Combustion, Kluwer Academic Publisher, 1996.

[5]Sorkin, R.E., *Dynamics and Thermodynamics of Solid-Propellant Rockets*, Wiener Bindery Ltd., Jerusalem, 1967.

[6]Shapiro, A.H., *The Dynamics and Thermodynamics of Compressible Fluid Flow*, Ronald Press, NY, Vol. I , 1953.

[7]Landay, L. D., and Lifshits, E. M., Fluid Mechanics, Pergamon, 1987.

[8]Hill, P., and Peterson, C., *Mechanics and Thermodynamics of Propulsion,* 2-rd ed.,,Addison-Wesley Publishing Company, Inc. New York, 1992.

[9]Bartz, D. R. , *Heat Transfer from Rapidly Accelerating Flow of Rocket Combustion Cases and from Heated Air,* in *Advances in Heat Transfer*, vol. 2, Hartnett, J. P. , and Irvine, T. F. Jr., eds., New York: Academic Press, 1965.

[10]*Handbook of Heat Transfer Application*, 2-rd ed, Rhsenow, W. M. , Hartnett, J. P. and Ganic, E. N. , eds., McGraw-Hill Book Company, New York, 1973.

Proceedings

[11]Flandro, G. A. Fischbach S., Majdalani J., French J., "Nonlinear Rocket Motor Stability Prediction: Limit Amplitude, Triggering, and Mean Pressure Shift", *AIAA 2004-4054, 40th AIAA Joint Propulsion Conference & Exhibit, July 2004*, Flodira.

[12]D. Luchinsky, V. Smelyanskiy, S. Osipov, and D. Timucin, and S. Lee, "Data management and decision support for the in-flight SRM", *AIAA-2007-2829 AIAA Infotech@Aerospace 2007 Conference and Exhibit, Rohnert Park*, California, May 7-10, 2007

[13]Osipov, V., Luchinsky, Smelyanskiy, V., Lee, S., Kiris, D., Timucin, "Bayesian Framework for In-Flight SRM Data Management and Decision Support", IEEE 2007 Aerospace Conference, Big Sky, March 2007.

[14]Smelyanskiy, V., Kiris, C., Osipov, V., Luchinsky, D., Timucin, D., and Uckun, S., "Solid Rocket Motor Health Management for Safe Space Flight", *AIAA-2006-6555, AIAA Guidance, Navigation, and Control Conference and Exhibit*, Keystone, Colorado, Aug. 21-24, 2006

[15]Sailta, M., "Verification of Spatial and Temporal Pressure Distribution in Segmented Solid Rocket Motors," *AIAA paper 89-0298, 27th Aerospace Science Meeting*, Reno, Nevada, Jan. 9-12, 1989.

[16]Young G., Bruck H.A., and Gowrisankaran S., "Modeling of Rocket Motor Ballistics for Functionally Graded Propellants", *Proceedings of the 39th JANNAF Combustion Meeting*, Colorado Springs, CO, December, 2003.

[17]Thompson, C. M., "Spacecraft Thermal Control, Design, and Operation," *AIAA Guidance, Navigation, and Control Conference*, CP849, Vol. 1, AIAA, Washington, DC, 1989, pp. 103-115.

[18]Chi, Y., (ed.), *Fluid Mechanics Proceedings*, SP-255, NASA, 1993.

[19]Morris, J. D. "Convective Heat Transfer in Radially Rotating Ducts," *Proceedings of the Annual Heat Transfer Conference*, edited by B. Corbell, Vol. 1, Inst. Of Mechanical Engineering, New York, 1992, pp. 227-234.

Reports, Theses, and Individual Papers

[20]Tauber, M. E., *A review of High-Speed, Convective, Head-Transfer Computation Methods*, NASA technical paper 2914, 1989.

[21]Chapman, G. T., and Tobak, M., "Nonlinear Problems in Flight Dynamics," NASA TM-85940, 1984.

Computer Software

[22]http://www.fluent.com.